Desalination and Water Treatment
www.deswater.com

doi: 10.5004/dwt.2017.21383

89 (2017) 250–257
September

Removal/separation of Co(II) ion from environmental sample solutions by $MnFe_2O_4$/bentonite nanocomposite as a magnetic nanomaterial

Arezoo Rahmani[a,b,*], Gholam Reza Karimi[a], Abasat Rahmani[b], Mehdi Hosseini[b,c], Ashkan Rahmani[d]

[a]Department of Mineral Processing, School of Engineering, IKIU, Qazvin, Iran, Tel. +98 24-36522283; email: arezu.rahmani@gmail.com (A. Rahmani), Tel. +98 281-8371111; email: gh.karimi@eng.ikiu.ac.ir (G.-R. Karimi)
[b]Research & Development Center, Calcimin Company, Zanjan, Iran, Tel. +98 24-36522283; email: abasat.rahmani@gmail.com (A. Rahmani), Tel. +98 24-36522242; email: mehdi.hosseini.znu@gmail.com (M. Hosseini)
[c]University of Applied Science, Calcimin Center, Dandi, Zanjan, Iran
[d]Department of Mining Engineering, School of Engineering, University of Zanjan, Zanjan, Iran, Tel. +98 24-33652283; email: ashkan6666@gmail.com (A. Rahmani)

Received 11 September 2016; Accepted 26 August 2017

ABSTRACT

$MnFe_2O_4$/bentonite nanocomposite was synthesized by chemical co-precipitation method. The prepared nanocomposite was characterized by X-ray diffraction (XRD), vibrating sample magnetometer (VSM) and scanning electron microscopy (SEM) techniques. The XRD results indicated the montmorillonite associated with quartz phases in the structure of $MnFe_2O_4$/bentonite nanocomposite synthesized. VSM was carried out to characterize the magnetic properties of the nanocomposite prepared. SEM images of the nanoadsorbent showed that nanocomposite has a uniform structure in the range of 50–200 nm in diameter. Adsorption characteristic of the synthesized nanocomposite was examined to evaluate adsorption of the cobalt(II) ion from aqueous sample solutions and at pH range of 4.5–5.0 the maximum amount of cobalt(II) ion was adsorbed. The maximum adsorption capacity of cobalt(II) was determined to be 22.42 mg g^{-1}. The results showed that nanocomposite has catalytic activity higher than the bentonite itself. The results obtained from the adsorption kinetic studies showed that adsorption behavior of cobalt(II) ion onto nanoadsorbent conformed to Langmuir isotherm model and pseudo-second-order kinetic.

Keywords: Co(II) ion; Removal/separation; Adsorption mechanism; $MnFe_2O_4$/bentonite nanocomposite; Environmental samples

1. Introduction

Heavy metal removal from water, groundwater and industrial wastewater are currently an important environmental concern. It is important to create awareness about the possible effects of increasing levels of environmental heavy metals pollutions on human health and the environment [1]. A great deal of effort has been devoted to the effective removal or separation of heavy metal ions from environmental matrices. Various treatment techniques available for the removal of heavy metals are as follows: adsorption, chemical precipitation, ion exchange, coagulation, reverse osmosis, electrolysis, membrane process, etc. [2–5]. Adsorption is universal, fast and applicable method for the removal of organic and inorganic pollutants even at low concentrations. Recent research focused on adsorbents such as activated carbons, zeolites, clays, biomass, chitosan, polymeric [6–8] and magnetic composite used to removal of heavy metals from industrial wastewater [9]. Natural clays are low-cost and readily available materials functioning as excellent cation exchangers. Clay and its various modifications have been extensively employed for the treatment

---

* Corresponding author.

of water and wastewater. Zeolites as one of the low-cost adsorbents showed capability to adsorb heavy metals. The use of zeolites for Co(II) removal was studied [10]. Different types of clays as low-cost adsorbents, for heavy metal removal have been reported [11,12] such as sepiolite clay for the removal of Co(II) ions from polluted [13]. Smectite clays such as bentonite and montmorillonite are fundamental soil components and are abundant in nature [14–17]. The adsorption capacity of clays results from a relatively high surface area and a net negative charge on their structure, which attracts and holds cations [18,19]. Bentonite has a 2:1 layer structure and it consists of alumina octahedral layer sandwiched between two silica tetrahedral layers [20]. Chemical modifications on clays with acids, bases, cationic surfactants and certain polyhydroxyl cations were conducted to improve their adsorption capacity [21]. It was reported that the intercalation of certain metal oxides on 2:1 clay minerals significantly led to an increase in the adsorption capacity [22].

The applications of magnetic particles to solve environmental pollutant problems were also considered. Magnetic particles and nanomaterials could be used to adsorb contaminants (such as $MnFe_2O_4$ azo dye) from aqueous or gaseous effluents and after adsorption process; the adsorbent could be easily separated from the medium [23]. Several materials such as magnetic porous ferro-spinel $MnFe_2O_4$ [24], magnetic $Co_{0.6}Fe_{2.4}O_4$ micro-particles as [25] and nano-magnetic iron oxide–nanosilicon oxide have been used and evaluated to removal of heavy metals [26].

In recent years, there are a growing interest in use of nanocomposite materials such as magnetic zeolite composite [27], polypyrolle Fe_3O_4-nanocomposite [28], amino functionlized-Fe_2O_3 nanoparticles [29], manganese oxide–incorporated ferric oxide nanocomposite [30], nanomagnetic iron oxide–nanosilicon oxide [31], SD/$MnFe_2O_4$ composite, a biosorbent [32], $MnFe_2O_4$/chitosan nanocomposites [33], $MnFe_2O_4$-graphenecomposite [34], and Clay ferrite nanocomposite ($MgFe_2O_4$ bentonite nanocomposite) [35] have been used for the removal of heavy metal from waste waters samples. Among the magnetic nanomaterials, bentonite/$MnFe_2O_4$ nanocomposite and montmorillonite/$CoFe_2O_4$ composite were used for removal of acid red and methylene blue.

In the present work, a nanocomposite of $MnFe_2O_4$/bentonite was successfully synthesized and characterized by several techniques and finally used as adsorbent for evaluation capability of removal/extraction of cobalt(II) ions from several environmental samples.

2. Materials and methods

2.1. Materials

Manganese(II) chloride ($MnCl_2$), ferric(III) chloride ($FeCl_3$) and cobalt sulfate heptahyrate ($CoSO_4.7H_2O$) were purchased from Merck (Darmstadt, Germany). The stock solution of cobalt(II) prepared from salt of $CoSO_4.7H_2O$ (1,000 mg L^{-1}). The required cobalt(II) solutions were diluted from stock solution. All reagents were prepared from analytical grade. Deionized water was used in all of experiments.

2.2. Instrumentation

A Metrohm digital pH-meter (model 692, Herisau, Switzerland) equipped with a glass-combination electrode was used for pH adjustment. The measurements of Co(II) ions were performed with a flame atomic absorption spectrometer (Thermo Electron Corporations Series) equipped with a hollow cathode lamp and a deuterium background corrector. The hollow cathode lamp of cobalt was operated at 4 mA and wavelength at 240.7 nm.

2.3. Synthesis of $MnFe_2O_4$/bentonite nanocomposite

$MnFe_2O_4$/bentonite magnetic nanocomposite was synthesized by co-precipitation method [36,37]. Briefly, 10 g of bentonite (200 mesh) was added into a solution containing manganese(II) chloride (0.02 mol) and ferric(III) chloride (0.04 mol) at room temperature (25°C). The pH adjusted by adding NH_3 (5 mol L^{-1}) or NaOH (0.1 mol L^{-1}) solution to pH of 10 and stirring was continued for 30 min. Next, the suspension was heated at temperature of 85°C–90°C for 2 h. The solution was cooled at room temperature, and the product (prepared magnetic nanocomposite) was repeatedly washed several times with distilled water. Finally, the obtained product was separated from water media and dried at 105°C for 2 h.

2.4. Analytical procedure

A 50 mL of sample solution containing Co(II) ions at different concentrations with 200 mg of adsorbent were mixed. Next, pH of sample solutions was adjusted by using 0.1 mol L^{-1} of HCl (1.0–3.0 range), 0.1 mol L^{-1} of acetic acid/sodium acetate (4.0–6.0 range) and 0.5 mol L^{-1} of NH_3 or 0.1 mol L^{-1} of NaOH (7.0–8.0 range). The mixture (cobalt(II) ions) was agitated in the mechanical shaker at 350 rpm for 10 min (or at different time intervals) at room temperature to create contact with adsorbent. After adsorption process, the mixture was filtered using Whatman filter paper. The amount of Co(II) ions remaining in the filtrated solution was measured using FAAS. The experiments were performed to evaluate the adsorption capacities of $MnFe_2O_4$/bentonite nanocomposite at different pH (2.0–8.0) and contact times. All the experiments were performed in triplicate. For regeneration studies, the adsorbent was centrifuged with 0.1 mol L^{-1} of NaOH solution.

The adsorbed amounts (q) of cobalt(II) ions were calculated by following equation (1):

$$q = \frac{(C_0 - C_e)V}{m} \tag{1}$$

where C_0 and C_e are the initial and equilibrium concentrations of cobalt(II) ions (mg L^{-1}), respectively, m is the mass of nanocomposite (g) and V is the volume of sample solution (L).

3. Results and discussion

3.1. Characterization of synthesized $MnFe_2O_4$/bentonite nanocomposite

The chemical composition/structure of $MnFe_2O_4$/bentonite and natural bentonite examined by X-ray diffraction (XRD) analysis. XRD results indicated natural bentonite has montmorillonite with free quartz structure and no any obvious crystalline peak, hence, Fe-O and Mn-O oxides in the $MnFe_2O_4$/bentonite nanocomposite exist mainly in the amorphous forms. The Fe and Mn components are complex and include $MnFe_2O_4$ (diffraction peaks at 18.1°, 29.7°, 35°, 42.5°, 52.8° and 61.9° 2θ) and furthermore spinel structure of $MnFe_2O_4$ has been verified (Fig. 1).

The morphology of natural bentonite and $MnFe_2O_4$/bentonite nanocomposite before and after adsorption process was evaluated by scanning electron microscopy (SEM; Figs. 2(a)–(c)) and obtained images showed that agglomeration of many micro fine particles in diameter of 50–200 nm for $MnFe_2O_4$/bentonite nanocomposite, which lead to a rough surface and porous and almost uniform structure and furthermore was evidence to high surface area of the resultant $MnFe_2O_4$/bentonite nanocomposite.

Evaluation of magnetic properties measurements was carried out at room temperature using a vibrating sample magnetometery (VSM). Fig. 3 shows the hysteresis loops of the $MnFe_2O_4$/bentonite nanocomposite. Under applied magnetic field and at room temperature, the nanocomposite exhibits a clearly hysteretic behavior. The product has high magnetic sensitivity due to the attraction toward the magnet in a short time. In addition, results showed that nanocomposite could be potentially used as a magnetic adsorbent.

3.2. Effect of contact time

The effect of contact time of adsorption of cobalt(II) onto bentonite and $MnFe_2O_4$/bentonite nanocomposite is shown in Fig. 4. For $MnFe_2O_4$/bentonite nanocomposite, amounts of Co(II) adsorbed is higher than (about 37.5%) the natural bentonite after 10 min contact time, which shows $MnFe_2O_4$/bentonite nanocomposite, exhibits an excellent adsorbent/catalyst.

The adsorption process could be divided into two steps, a quick step and a slow one. In the first step, the adsorption rate was fast, and 97% of the equilibrium adsorption capacity was achieved within 10 min. In the subsequent step, the adsorption was slow and reached equilibrium at 1 h. It is obvious from the fact that a large number of surface sites are available for adsorption at the initial stages, and after a lapse of time, the remaining surface sites are difficult to be occupied because of the repulsion between the solute molecules of the solid and the bulk phase occurred. This is due to higher contact between the sorbent surface and Co ions.

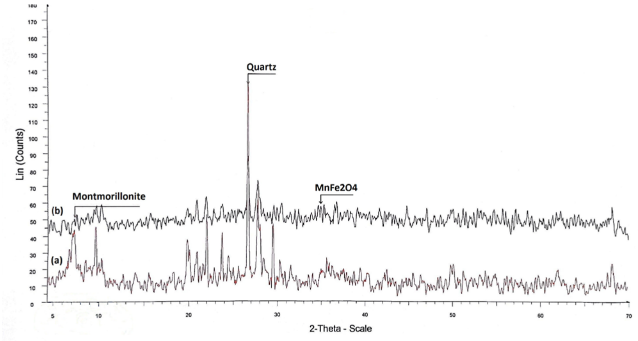

Fig. 1. XRD pattern of (a) Bentonite and (b) spinel $MnFe_2O_4$/bentonite nanocomposite.

3.3. Adsorption isotherm

Adsorption capacity and adsorption behavior of Co(II) on $MnFe_2O_4$/bentonite nanocomposite can be illustrated by

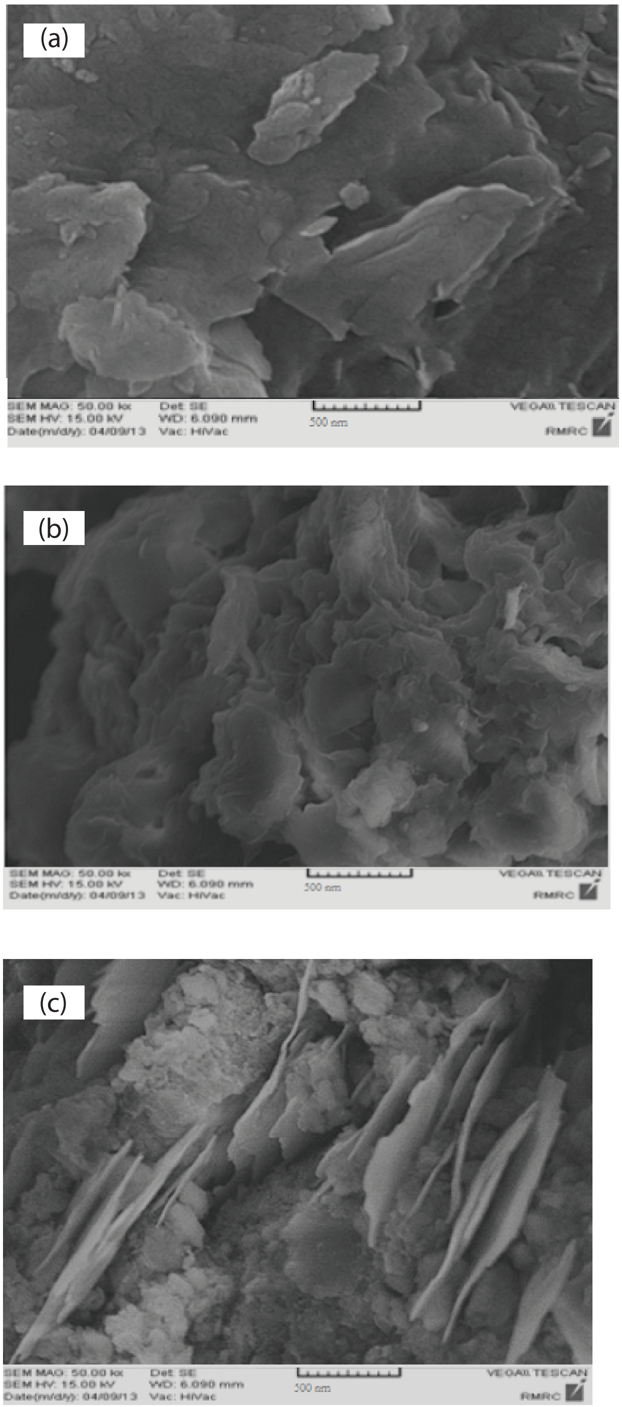

Fig. 2. SEM images of (a) natural bentonite, (b) $MnFe_2O_4$/bentonite nanocomposite before adsorption of cobalt(II) ion and (c) $MnFe_2O_4$/bentonite nanocomposite after adsorption of Co(II) ions.

adsorption isotherm. Data from the adsorption isotherms were modeled using the Langmuir, Freundlich and Temkin isotherm models with the resulting isotherm constants presented in Table 1.

The Langmuir isotherm theory is based on the assumption of adsorption on a homogenous surface [38]. The Langmuir equation can be written in the following equation:

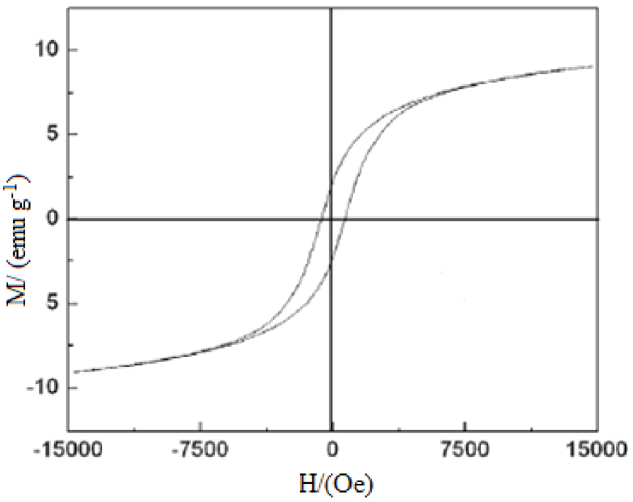

Fig. 3. Magnetic hysteresis curve for the $MnFe_2O_4$/bentonite nanocomposite.

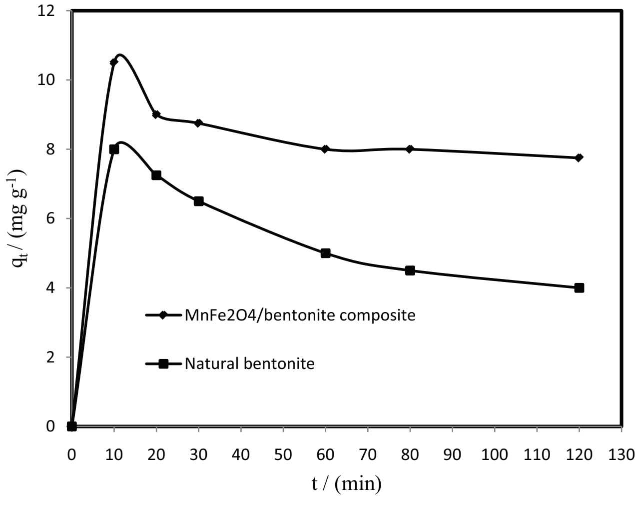

Fig. 4. Effect of contact time of adsorption Co(II) onto $MnFe_2O_4$/bentonite nanocomposite (50 mL of Co(II) 100 mg L^{-1}, initial concentration 100 mg L^{-1}, pH = 4.5–5.0 and 200 mg of adsorbent).

$$q_e = q_{\max} K_L C_e/(1 + K_L C_e) \tag{2}$$

The linearized form of Langmuir equation can be written as follows (Fig. 5(a)):

$$C_e/q_e = 1/q_{\max} K_L + C_e/q_{\max} \tag{3}$$

where q_e is the solid-phase equilibrium concentration (mg g^{-1}); C_e is the liquid equilibrium concentration of Co(II) in solution (mg L^{-1}); K_L is the equilibrium constant related to the affinity of binding sites (L mg^{-1}); and $q_{\max}$ is the maximum amount of the Co(II) per unit weight of adsorbent for complete monolayer coverage.

The Freundlich isotherm describes adsorption where the adsorbent has a heterogeneous surface with adsorption sites that have different energies of adsorption [39]. The energy of adsorption varies as a function of the surface coverage (q_e) and is represented by Freundlich constant K_F (L g^{-1}) in Eq. (4):

$$q_e = K_F C_e^{\,n} \tag{4}$$

where K_F is roughly an indicator of the adsorption capacity and n is the heterogeneity factor which has a lower value for more heterogeneous surfaces. In most references, Freundlich adsorption Eq. (4) may be also expressed as Eq. (5) (Fig. 5(b)):

$$\ln q_e = \ln K_F + 1/n \ln C_e \tag{5}$$

The Temkin isotherm model assumes that heat of adsorption (function of temperature) of all molecules in the layer would decrease linearly with the coverage of molecules [40]. The nonlinear form of Temkin may be also expressed as Eq. (6) (Fig. 5(c)):

$$q_e = B_T \ln A + B_T \ln C_e \tag{6}$$

where ($RT/b = B_T$) and T is the absolute temperature in Kelvin, R is the universal gas constant, b is related to the heat of adsorption and A is the equilibrium-binding constant corresponding to the maximum binding energy.

All the R^2 value, and the constants obtained for the models from Table 1 show that the Langmuir isotherm is the suitable equation to describe the adsorption equilibrium of Co(II) on the $MnFe_2O_4$/bentonite nanocomposite.

3.4. Kinetic of adsorption

In order to predict adsorption kinetic model of cobalt solutions, pseudo-first-order and pseudo-second-order kinetic models were applied to the data. The

Table 1
Langmuir, Freundlich and Temkin isotherms constant for adsorption of Co(II) onto $MnFe_2O_4$/bentonite nanocomposite

Type of adsorbent	Langmuir model			Freundlich model			Temkin model		
	$q_{\max}$ (mg g^{-1})	K_1 (L g^{-1})	R^2	K_f (mg g^{-1})	$1/n$	R^2	B_T (J mol^{-1})	A (L g^{-1})	R^2
$MnFe_2O_4$/bentonite, nanocomposite	22.42	90.9	0.95	14.8	3.55	0.79	3.25	114.6	0.89

pseudo-first-order model assumes that the rate of change of solute uptake with time is directly proportional to difference in saturation concentration and amount of solid uptake with time [41–42]. The linear form of pseudo-first-order model could be expressed as Eq. (7):

$$\ln(q_e - q_t) = \ln q_e - k_1 t \tag{7}$$

where q_e and q_t are the amounts of Co(II) adsorbed per unit mass of the adsorbent (mg g^{-1}) at equilibrium and time t, respectively, and k_1 is the rate constant of adsorption (min^{-1}). When $\ln(q_e - q_t)$ was plotted against time, a straight line should be obtained with a slope of $-k_1$, if the first-order kinetics is valid.

The pseudo-second-order model has the following form:

$$t/q_t = t/q_e + 1/(k_2\, q_e^2) \tag{8}$$

where q_e and q_t represent the amount of Co(II) adsorbed (mg g^{-1}) at equilibrium and at any time, k_2 in the rate constant of the pseudo-second-order equation (g mg^{-1} min^{-1}). A plot of t/q_t vs. time (t) would yield a line with a slope of $1/q_e$ and an intercept of $1/(k_2 q_e^2)$, if the second-order model is a suitable expression.

The plot between $\ln(q_e - q_t)$ vs. time t shows the pseudo-first-order model and the plot of t/q_t vs. time t shows the pseudo-second-order model (Figs. 6 and 7).

The kinetic model with a higher correlation coefficient R^2 was selected as the most suitable one. It was found that application of pseudo-second-order kinetics provides better correlation coefficient of experimental data than the pseudo-first-order model for the Co(II) onto nanocomposite adsorbent. The good correlation coefficients were obtained

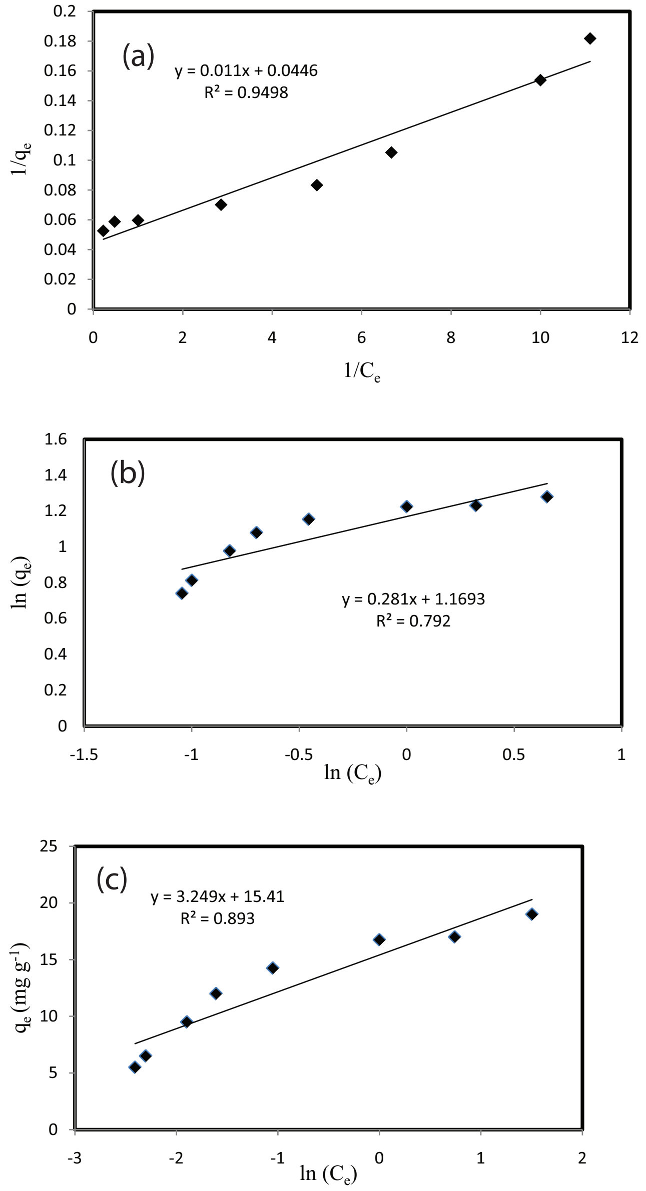

Fig. 5. (a) Langmuir plot for Co(II) on the MnFe$_2$O$_4$/bentonite nanocomposite (50 mL Co(II) solution, initial concentration 100 mg L^{-1}, pH = 4.5–5.0 and 200 mg of adsorbent); (b) Freundlich plot for Co(II) on the MnFe$_2$O$_4$/bentonite nanocomposite (50 mL Co(II) solution, initial concentration 100 mg L^{-1}, pH = 4.5–5.0 and 200 mg of adsorbent); (c) Temkin plot for Co(II) on the MnFe$_2$O$_4$/bentonite nanocomposite (50 mL Co(II) solution, initial concentration 100 mg L^{-1}, pH = 4.5–5.0, and 200 mg of adsorbent).

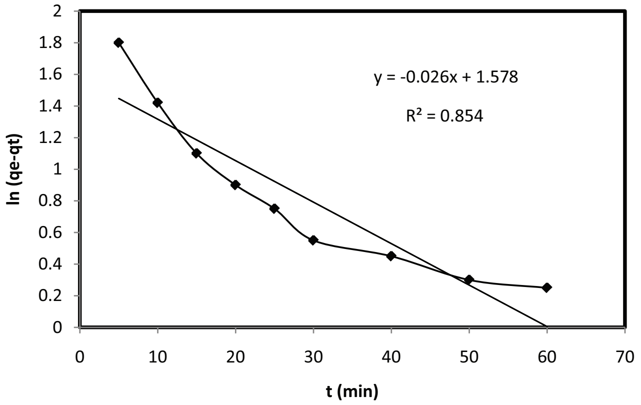

Fig. 6. Pseudo-first-order kinetics for adsorption of Co(II) on MnFe$_2$O$_4$/bentonite nanocomposite (50 mL Co(II) solution, initial concentration 100 mg L^{-1}, pH = 4.5–5.0 and 200 mg of adsorbent).

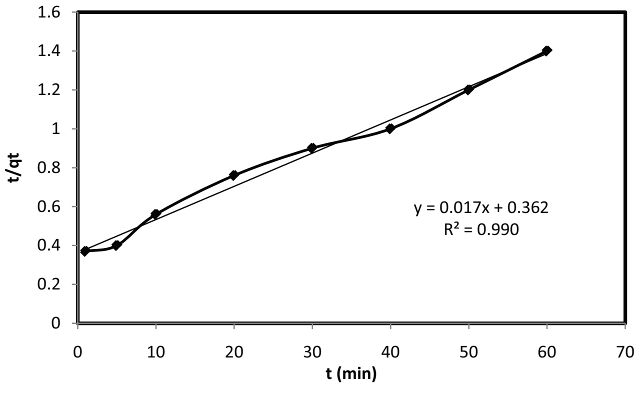

Fig. 7. Pseudo-second-order kinetics for adsorption of Co(II) on MnFe$_2$O$_4$/bentonite nanocomposite (50 mL Co(II) solution, initial concentration 100 mg L^{-1}, pH = 4.5–5.0, and 200 mg of adsorbent).

by fitting the experimental data to Eq. (6), indicating that the adsorption kinetic on $MnFe_2O_4$/bentonite is pseudo-second order. The values of rate constant were calculated from the slope of Figs. 6 and 7 are represented in Table 2.

3.5. Effect of pH of sample solution

The effect of pH on the adsorption of Co(II) onto $MnFe_2O_4$/bentonite nanocomposite was studied by varying the pH of solution from 2.0 to 8.0. The experiments were carried out for 50 mL of Co(II) ions with initial concentration of 100 mg L^{-1} and 200 mg of adsorbent. Results showed that amount of Co(II) ions adsorbed on adsorbent increased when pH value was increased.

It is evident that the amount of adsorption strongly depends on pH solution of media. The adsorption percentage of Co(II) by $MnFe_2O_4$/bentonite nanocomposite is increased with the increase of the pH value, and the maximum uptake of the Co(II) takes place at around pH of 8.0 (Fig. 8). It was noticed that when the pH value was more than 5, the adsorption amount increased dramatically; this was attributed to the fact that heavy metal ions such as cobalt (II) ions started to precipitate (to form metal hydroxide, $Co(OH)_2$) leading to the reduction of the metal ions in the aqueous solution at higher pH value. However, pH range of 4.5–5.0 was selected as optimum amount that yield a good recovery.

Table 2
Kinetics parameters for the adsorption of Co(II) onto $MnFe_2O_4$/bentonite nanocomposite

First order		Second order	
R^2	K_1 (min^{-1})	R^2	K_2 (g mg^{-1} min^{-1})
0.854	0.0262	0.990	1.06×10^{-3}

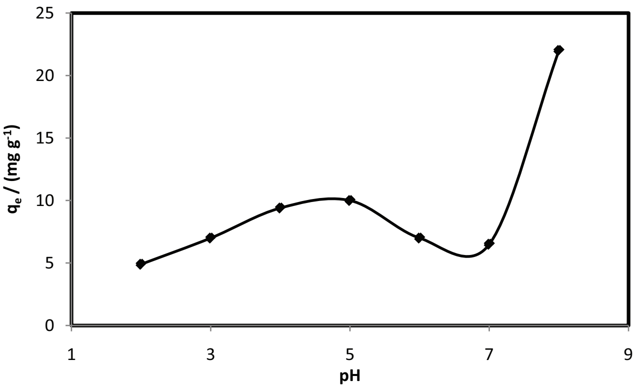

Fig. 8. Effect of pH on adsorption of Co(II) onto $MnFe_2O_4$/bentonite nanocomposite (50 mL Co(II) solution, initial concentration 100 mg L^{-1}, pH = 4.5–5.0, and 200 mg of adsorbent).

3.6. Comparison of capability of present method vs. similar work

The removal of Co(II) ions from different aqueous media by different adsorbents has been studied extensively, and capability of $MnFe_2O_4$/bentonite nanocomposite rather than common adsorbents reported previously are comprised in Table 3.

It could be seen that adsorption capacities of present nanocomposite was higher than other ones and indicate that prepared nanocomposite has great ability and potential in the removal of Co(II) ions from aqueous sample solutions.

4. Conclusions

Results showed that $MnFe_2O_4$/bentonite has magnetic properties, nanostructure and high adsorption capacity (22.42 mg g^{-1}). Separation/removal of cobalt was fast, simple and effective procedure. Synthesize of $MnFe_2O_4$/bentonite nanocomposite was carried out by chemical co-precipitation method and characterized by SEM, XRD and VSM techniques. Removal of Co(II) ion was highly dependent on pH of sample solution and pH range of 4.5–5.0 was selected as optimum amount. Adsorption experiments revealed that the nanocomposite has much higher catalytic activity rather than the bentonite. Langmuir isotherm is the suitable model to describe the adsorption equilibrium and good correlation coefficients were obtained by fitting the experimental data indicating that adsorption kinetic of Co(II) on $MnFe_2O_4$/bentonite is pseudo-second order.

Acknowledgments

The authors express their appreciation to the Graduate School and Research & Development of Calcimin Company for financial support of this work.

Table 3
Comparison of present work for adsorption of Co(II) ion with previous works

Adsorbent	Co(II) Conc. (mg L^{-1})	Adsorbent dose (g L^{-1})	Reaction time (h)	Capacity (mg g^{-1})	Ref.
Kaolinite	2,400	1.0	2	0.9	[44]
Al-pillared bentonite clay	10,000	1.0	24	38.61	[18]
Sepiolite	58.9	50	2	7.57	[13]
Chitosan–montmorillonite	825	4	12	150	[45]
Fe-Mn binary	5.89	0.1	24	20.25	[43]
Amination graphene oxide nanocomposite	–	0.3	12	116.35	[46]
$MnFe_2O_4$/bentonite nanocomposite	100	40	0.16	22.42	Present work

References

[1] M.V. Liao, Y. Chien, K. Ou. Tseng, Assessment of heavy metal bioavailability in contaminated sediments and soils using green fluorescent protein-based bacterial biosensors, Environ. Pollut., 142 (2006) 17–23.

[2] V.K. Gupta, Application of low-cost adsorbents for dye removal: a review, Environ. Manage., 90 (2009) 2313–2342.

[3] V.K. Gupta, A. Rastogi, V. Saini, N. Jain, Biosorption of copper (II) from aqueous solutions by Spirogyra species, J. Colloid Interface Sci., 296 (2006) 59–63.

[4] A. Heidari, H. Younesi, Z. Mehraban, Removal of Ni(II), Cd(II), and Pb(II) from a ternary aqueous solution by amino functionalized mesoporous and nano mesoporous silica, Chem. Eng. J., 153 (2009) 70–79.

[5] Y. Pang, G. Zeng, L. Tang, Y. Zhang, Y. Liu, X. Lei, PEI-grafted magnetic porous powder for highly effective adsorption of heavy metal ions, Desalination, 281 (2011) 278–284.

[6] G. Crini, Recent developments in polysaccharide-based materials used as adsorbents in wastewater treatment, Progr. Polym. Sci., 30 (2005) 38–70.

[7] V.N. Tirtom, A. Dincer, S. Becerik, Comparative adsorption of Ni(II) and Cd(II) ions on epichlorohydrin crosslinked chitosan–clay composite beads in aqueous solution, Chem. Eng. J., 197 (2012) 379–386.

[8] W.S. Wan Ngah, L.C. Teong, M.A.K.M. Hanafiah, Adsorption of dyes and heavy metal ions by chitosan composites: a review, Carbohydr. Polym., 83 (2010) 1446–1456.

[9] A.Z.M. Badruddoza, Z.B.Z. Shawon, et al., Fe_3O_4/cyclodextrin polymer nano composites for selective heavy metals removal from industrial wastewater, Carbohydr. Polym., 91 (2012) 322–332.

[10] J.S. Kim, M.A. Keane, The removal of iron and cobalt from aqueous solutions by ion exchange with Na–Y–Zeolite batch, semibatch and continuous operation, J. Chem. Technol. Biotechnol., 77 (2002) 633–640.

[11] H. Katsumata, S. Kaneco, K. Inomata, K. Itoh, K. Funasaka, K. Masuyama, T. Suzuki, K. Ohta, Removal of heavy metals in rinsing wastewater from plating factory by adsorption with economical viable materials, J. Environ. Manage., 69 (2003) 187–191.

[12] M.G. Fonseca, M.M. Oliveira, L.N.H. Arakaki, Removal of cadmium, zinc, manganese and chromium cations from aqueous solution by a clay mineral, J. Hazard. Mater., 137 (2006) 288–292.

[13] M. Kara, H. Yuzer, E. Sabah, M.S. Celik, Adsorption of cobalt from aqueous solution onto sepiolite, Water Res., 37 (2003) 224–232.

[14] G.W. Beall, The use of organo-clays in water treatment, Appl. Clay Sci., 24 (2003) 11–20.

[15] L. Yuan, D. Huang, W. Guo, Q. Yang, J. Yu, TiO_2/montmorillonite nanocomposite for removal of organic pollutant, Appl. Clay Sci., 53 (2011) 272–278.

[16] D.W. Cho, C.M. Chon, B.H. Jeon, Y. Kim, M.A. Khan, H. Song, The role of clay minerals in the reduction of nitrate in groundwater by zero-valent iron, Chemosphere, 81 (2010) 611–616.

[17] H.H. Murray, Traditional and new applications for kaolin, smectite and palygorskite: a general overview, Appl. Clay Sci., 17 (2000) 207–222.

[18] D.M. Manohar, B.F. Noeline, T.S. Anirudhan, Adsorption performance of Al-pillared bentonite clay for the removal of Co(II) from aqueous phase, Appl. Clay Sci., 31 (2006) 194–206.

[19] A. Khenifi, Adsorption study of an industrial dye by organic clay, Adsorption, 13 (2007) 149–158.

[20] L.C.A. Oliveir, Clay-iron oxide magnetic composites for the adsorption of contaminants in water, Appl. Clay Sci., 22 (2003) 169–177.

[21] T. Vengris, R. Binkiene, A. Sveikauskaite, Nickel, copper and zinc removal from wastewater by modified clay sorbent, Appl. Clay Sci., 18 (2001) 183–190.

[22] B. Lothenbach, G. Furrer, R. Schulin, Immobilisation of heavy metals by polynuclear aluminium and montmorillonite compounds, Environ. Sci. Technol., 31 (1997) 1452–1462.

[23] R. Wu, J. Qu, Removal of water-soluble azo dye by the magnetic material $MnFe_2O_4$, J. Chem. Technol. Biotechnol., 80 (2005) 20–27.

[24] Y. Ren, N. Li, J. Feng, T. Luan, Q. Wen, Z. Li, M. Zhang, Adsorption of Pb(II) and Cu(II) from aqueous solution on magnetic porous ferrospinel $MnFe_2O_4$, J. Colloid Interface Sci., 367 (2012) 415–421.

[25] S. Duan, R. Tang, Z. Xue, X. Zhang, Y. Zhao, W. Zhang, J. Zhang, B. Wang, S. N. Zeng, D. Sun, Effective removal of Pb(II) using magnetic $Co^0.6Fe_2.4O_4$ micro-particles as the adsorbent: synthesis and study on the kinetic and thermodynamic behaviors for its adsorption, Colloids Surf., A, 469 (2015) 211–223.

[26] M.E. Mahmoud, M.S. Abdelwahab, E.M. Fathallah, Design of novel nano-sorbents based on nano-magnetic iron oxide–bound-nano-silicon oxide–immobilized-triethylenetetramine for implementation in water treatment of heavy metals, Chem. Eng. J., 223 (2013) 318–327.

[27] K.N. Barquist, Synthesis and environmental adsorption applications of functionalized zeolites and iron oxide/zeolite composites, PhD thesis. Available at: http://ir.uiowa.edu/etd/334.

[28] M. Bhaumik, K. Setshedi, A. Maity, M.S. Onyango, Chromium (VI) removal from water using fixed bed column of polypyrrole/Fe_3O_4 nanocomposite, Sep. Purif. Technol., 110 (2013) 11–19.

[29] Y.M. Hao, C. Man, Z.B. Hu, Effective removal of Cu (II) ions from aqueous solution by amino functionalized magnetic nanoparticles, J. Hazard. Mater., 184 (2010) 392–399.

[30] A. Ghosh, M. Pal, K. Biswas, U. C. Ghosh, B. Manna, Manganese oxide incorporated ferric oxide nanocomposites (MIFN): a novel adsorbent for effective removal of Cr(VI) from contaminated water, J. Water Proc. Eng., 7 (2015) 176–186.

[31] M.E. Mahmoud, M.S. Abdelwahab, E.M. Fathallah, Design of novel nano-sorbents based on nano-magnetic iron oxide–bound-nano-silicon oxide–immobilized-triethylenetetramine for implementation in water treatment of heavy metals, Chem. Eng. J., 223 (2013) 318–327.

[32] M.S. Podder, C.B. Majumder, SD/$MnFe_2O_4$ composite, a biosorbent for As(III) and As(V) removal from wastewater: optimization and isotherm study, J. Mol. Liquids, 212 (2015) 382–404.

[33] Y. Xiao, H. Liang, Z. Wang, $MnFe_2O_4$/chitosan nanocomposites as a recyclable adsorbent for the removal of hexavalent chromium, Mater. Res. Bull., (2013) 3910–3915.

[34] S. Chella, P. Kollu, Eswara Vara P R Komarala, S. Doshi, M. Sarany, S. Felix, R. Ramachandran, P. Saravanan, V.L. Koneru, V. Venugopal, S.K. Jeong, A.N. Grace, Solvo thermal synthesis of $MnFe_2O_4$-graphene composite-investigation of its adsorption and antimicrobial properties, Appl. Surf. Sci., 327 (2015) 27–36.

[35] M. Kaur, M. Singh, S.S. Mukhopadhyay, D. Singh, M. Gupta, Structural, magnetic and adsorptive properties of clay ferrite nanocomposite and its use for effective removal of Cr (VI) from water, J. Alloys Comp., 653 (2015) 202–211.

[36] S. Hashemian, $MnFe_2O_4$/bentonite nano composite as a novel magnetic material for adsorption of acid red 138, Afr. J. Biotechnol., 9 (2010) 8667–8671.

[37] A. Lunhong, You Zhou, J. Jiang, Removal of methylene blue from aqueous solution by montmorillonite/$CoFe_2O_4$ composite with magnetic separation performance, Desalination, 266 (2011) 72–77.

[38] M. Hosseini, N. Dalali, A. Karimi, K. Dastanra, Solid phase extraction of copper, nickel, and cobalt in water samples after extraction using surfactant coated alumina modified with indane-1,2,3-trione 1,2-dioxime and determination by flame atomic absorption spectrometry, Turk. J. Chem., 34 (2010) 905–814.

[39] C.H. Yang, Statistical mechanical study on the Freundlich isotherm equation, J. Colloid Interface Sci., 2008 (1998) 379–387.

[40] C. Aharoni, M. Ungarish, Kinetics of activated chemisorption. Theoretical models, J. Chem. Soc., 73 (1977) 456–464.

[41] Y.S. Ho, Review of second-order models for adsorption systems, J. Hazard. Mater., 136 (2006) 681–689.

[42] Y.S. Ho, Citation review of Lagergren kinetic rate equation on adsorption reactions, Scientometr., 59 (1977) 171–177.

[43] L. Jiang, S. Xiao, J. Chen, Removal behavior and mechanism of Co(II) on the surface of Fe–Mn binary oxide adsorbent, Colloids Surf., A, 479 (2015) 1–10.

[44] O. Yavuz, Y. Altunkaynak, F.G. Uze, Removal of copper, nickel, cobalt and manganese from aqueous solution by kaolinite, Water Res., 37 (2003) 948–952.

[45] H. Wang, H. Tang, Z. Liu, X. Zhang, Removal of Co(II) ion from aqueous solution by chitosan–montmorillonite, J. Environ. Sci., 26 (2014) 1879–1884.

[46] F. Fang, L. Kong, J. Huang, S. Wu, K. Zhang, X. Wang, B. Sun, Z. Jin, J. Wang, X. Huang, J. Liu, Removal of cobalt ions from aqueous solution by an amination graphene oxide nanocomposite, J. Hazard. Mater., 270 (2014) 1–10.